S1 Additional information

In this section, additional information regarding Ural (discussed in Sect. 5.1) and Scandinavian (discussed in Sect. 5.2) events, respectively, such as event ranking, information about event classification (Sect. 4), trajectory calculations and blocking information are provided per event in Table S1 and Table S3. Furthermore, information regarding maximum heating of blocking trajectories, such as the relative contribution of the heated trajectories in the main heating domain and time of peak heating, and regarding cyclone activity (Sect. 6) are given in Table S2 and Table S4 for Ural and Scandinavian events, respectively.

Table S1: Additional information for each Ural event (30 events, 28 blocks) analyzed in Sect. 5 - part 1. Event ranking: event number ordered by extremeness (Nr), High-Arctic area-averaged T2m anomaly [K] (Tano) at the peak of each event. Cluster classification: Event cluster [U = Ural, S = Scandinavian or US = mixed cluster for both Ural and Scandinavian block] (Cluster), time lag of peak Ural or Scandinavian sector fraction within six days prior to the warm event [day] (lag), Ural or Scandinavian sector fraction corresponding to the previous lag (Sec. frac.). Trajectory calculation: time lag of peak Ural or Scandinavian sector fraction within days 3 to 1 prior to the warm event used for trajectory initialization [day] (lag), Ural or Scandinavian sector fraction corresponding to the previous lag (Sec. frac.), total number of trajectories computed from the block (Count), percentage of all trajectories belonging to the heating regime H based on 6-day trajectories (H). Block-information: unique blocking ID (ID), whole duration of the block [h] (dur.) and D-index, as defined by Eq. (1) (D-idx). Events are sorted by time.

Event ranking		Cluster classification			Trajectory calculation				Block-information		
Nr	**Tano**	**Cluster**	**lag (d)**	**Sec. frac.**	**lag (d)**	**Sec. frac.**	**Count**	**H (%)**	**ID**	**dur. (h)**	**D-idx**
50	6.17	U	0	0.3	-1	0.17	836	76	412	7.25	0.24
45	6.42	U	0	0.45	-1	0.25	3047	57	267	10.75	0.63
43	6.55	US	-1	0.57	-1	0.57	7955	80	418	19.75	0.37
38[1]	6.89	U	-4	0.69	-3	0.61	4077	54	419	18.0	0.46
29	7.47	U	-3	0.58	-3	0.58	5532	69	300	7.75	0.71
5[2]	9.58	U	0	0.28	-1	0.24	2151	66	325	17.5	0.09
12	9.15	U	-2	0.3	-2	0.3	3682	71	364	41.5	0.07
14	8.97	U	-1	0.39	-1	0.39	1668	25	**354**	23.75	0.44
8	9.29	U	-6	0.39	-1	0.31	466	1	**354**	23.75	0.99
42	6.66	US	-1	0.73	-1	0.73	3499	59	403	15.0	0.4
32	7.32	US	-3	0.45	-3	0.45	5753	72	414	17.75	0.55
2	11.61	U	-3	0.63	-3	0.63	4522	59	445	24.75	0.57
30	7.37	U	-4	0.24	-3	0.2	3479	73	394	36.5	0.94
7[3]	9.31	US	-2	0.48	-2	0.48	3694	38	460	58.75	0.19
4	11.03	U	-4	0.43	-3	0.42	2375	45	332	15.0	0.57
36[2]	7.05	U	0	0.43	-2	0.33	1494	58	401	25.75	0.14
13	9.11	U	-6	0.57	-2	0.54	3395	44	435	20.0	0.94
33	7.14	US	-3	0.58	-3	0.58	3676	33	266	15.0	0.43
22	8.35	US	-1	0.72	-1	0.72	6340	58	294	10.5	0.48
17	8.66	US	-2	0.49	-2	0.49	3166	76	424	18.0	0.51
23[2]	8.16	US	-2	0.67	-2	0.67	3452	64	436	27.25	0.7
9	9.21	US	0	0.4	-1	0.24	1750	73	**400**	6.0	0.12
1	11.83	U	-5	0.49	-3	0.29	1062	5	**400**	6.0	0.96
49[1]	6.17	U	0	0.41	-1	0.36	4021	74	443	46.25	0.16
19	8.55	US	-5	0.4	-3	0.17	2799	40	422	13.75	0.56
18	8.63	U	-3	0.32	-3	0.32	1359	81	470	13.0	0.85
40	6.79	US	-4	0.39	-3	0.31	967	22	494	5.25	0.9
31	7.36	U	-3	0.57	-3	0.57	5581	54	364	38.25	0.82
15[2]	8.95	US	-1	0.82	-1	0.82	3261	32	432	12.5	0.7
3	11.23	U	-6	0.36	-1	0.33	2346	67	236	19.0	0.8

Geographical masks: [1] $\geq 60^\circ$ N, [2] $\geq 60^\circ$ N & 0-180° E, [3] $\geq 60^\circ$ N & 50-180° E

Table S2: Additional information for each Ural event analyzed in Sect. 5 and Sect. 6 - part 2. Event ranking with event number (Nr) and date (Date). Maximum heating for heated trajectories: Relative percentages of all heated trajectories experiencing maximum heating within the main domain (A), peak time lag of maximum heating for blocking trajectories experiencing heating in the main domain A and for all heated trajectories relative to trajectory initialization [day] (lag A and lag all, respectively). Number of cyclones: within the northwest Atlantic sector (C) during a 5-day window between lags −6 to −1 days relative to trajectory initialization (C, 5d) and above 80° N during a 3-day window between lags −3 to 0 days with respect to each warm event (HA, 3d). Events are sorted by time.

Event ranking		Maximum heating for heated trajectories			Nr. of cyclones	
Nr	**Date**	**A (%)**	**lag A (day)**	**lag all (day)**	**C, 5d**	**HA, 3d**
50	(1980, 3, 15, 12)	77	-2.75	-2.75	4	2
45	(1982, 11, 30, 12)	96	-3	-3	5	3
43	(1983, 3, 3, 12)	91	-2	-2	5	3
38	(1984, 2, 5, 12)	94	-5	-5	4	2
29	(1984, 12, 20, 12)	72	-1	-1	5	3
5	(1985, 1, 1, 12)	0	nan	-3.25	6	1
12	(1986, 12, 15, 12)	86	-2.5	-2.5	4	2
14	(1990, 1, 10, 12)	96	-5.5	-5.5	5	2
8	(1990, 1, 23, 12)	17	-4	-5.5	5	2
42	(1990, 2, 6, 12)	78	-6	-6	4	1
32	(1990, 2, 21, 12)	23	-6	-5	5	0
2	(1992, 3, 18, 12)	49	-4	-3.5	6	2
30	(1995, 2, 13, 12)	81	-5	-5	6	1
7	(1997, 3, 10, 12)	50	-1.5	-1.5	6	2
4	(2000, 1, 1, 12)	34	-4.75	-4.25	7	1
36	(2000, 2, 14, 12)	69	-2.5	-2.5	7	1
13	(2000, 3, 18, 12)	22	-4	-4	6	1
33	(2001, 11, 29, 12)	70	-2.5	-5.5	2	2
22	(2002, 12, 8, 12)	71	-2.5	-2.5	4	2
17	(2005, 1, 28, 12)	50	-2.75	-3	7	2
23	(2005, 2, 20, 12)	71	-3.5	-3.5	2	2
9	(2006, 1, 17, 12)	77	-2.5	-2.5	4	4
1	(2006, 1, 24, 12)	90	-4.25	-4.25	4	2
49	(2011, 2, 15, 12)	94	-3.5	-3.5	5	2
19	(2012, 1, 18, 12)	71	-4.25	-4.25	4	3
18	(2014, 2, 14, 12)	76	-3.5	-3.5	6	1
40	(2015, 3, 8, 12)	25	-5.75	-2	3	0
31	(2016, 1, 28, 12)	85	-6	-6	6	1
15	(2016, 2, 24, 12)	25	-5.25	-5.25	3	2
3	(2016, 11, 16, 12)	63	-3.5	-3.5	5	2

Table S3: Same as in S1 but for Scandinavian events (10 events, 11 blocks) analyzed in Sect. 5. The two blocks for Event 24, shown by "a" and "b" refer to the two blocks found to be associated with Event 24, where "a" is the reference block used for the cyclone analysis presented in Sect. 6.

Event ranking		Cluster classification			Trajectory calculation				Block-information		
Nr	**Tano**	**Cluster**	**lag [d]**	**Sec. frac.**	**lag [d]**	**Sec. frac.**	**Count**	**H [%]**	**ID**	**dur. [h]**	**D-idx**
42	6.66	US	0	0.71	-1	0.46	4398	61	411	8.0	0.09
32	7.32	US	-5	0.29	-1	0.22	4321	44	429	5.5	0.18
6	9.47	S	-4	0.54	-3	0.49	3490	42	325	9.0	0.78
37[1]	7.01	S	0	0.44	-1	0.24	3646	76	470	6.75	0.26
10	9.21	S	-4	0.33	-3	0.29	1291	83	266	15.0	0.9
28	7.6	S	-1	0.66	-1	0.66	3709	52	299	10.0	0.5
19	8.55	US	-3	0.44	-3	0.44	2893	36	433	5.25	0.81
24a	8.05	S	0	0.39	-3	0.31	1492	61	451	9.75	0.95
24b	8.05	S	0	0.39	-1	0.15	858	62	470	13.0	0.08
40	6.79	US	0	0.35	-1	0.23	2928	71	500	5.0	0.45
16	8.9	S	-3	0.54	-3	0.54	3229	69	311	5.25	0.62

Geographical mask: [1] $< 73^\circ$ N

Table S4: Same as in S2 but for Scandinavian events as analyzed in Sect. 5 and Sect. 6. The two blocks for Event 24, shown by "a" and "b" refer to the two blocks found to be associated with Event 24, where "a" is the reference block used for the cyclone analysis presented in Sect. 6.

Event ranking		Maximum heating for heated trajectories			Nr. of cyclones	
Nr	**Date**	**A (%)**	**lag A (day)**	**lag all (day)**	**C, 5d**	**HA, 3d**
42	(1990, 2, 6, 12)	60	-1	-1	4	1
32	(1990, 2, 21, 12)	52	-2	-3	5	0
6	(1990, 12, 28, 12)	81	-6	-5.75	4	2
37	(1994, 2, 13, 12)	61	-1	-1	3	2
10	(2001, 12, 6, 12)	50	-2	-5	6	0
28	(2006, 1, 8, 12)	62	-3.5	-3.5	4	2
19	(2012, 1, 18, 12)	97	-5	-5	4	3
24a	(2014, 2, 2, 12)	42	-6	-6	3	1
24b	(2014, 2, 2, 12)	44	-1	-1.25	-	-
40	(2015, 3, 8, 12)	71	-1	-1	3	0
16	(2016, 12, 23, 12)	60	-3.75	-3.75	6	1

S2 Investigation of Ural blocking heated trajectories with additional pressure criteria

In this section, we will provide a further analysis on a sub-selection of the heated trajectories initialized from the Ural blocks related to 30 events (as analysed in Sect. 5.1), based on additional pressure criterion. The pressure criterion is motivated by the definition of warm conveyor belts (WCBs, Wernli and Davies, 1997; Madonna et al., 2014), described as air parcels started from the lower troposphere (below 790 hPa) and experiencing rapid ascent (more than 600 hPa within 48-hours). As discussed in the introduction of the main article, WCBs are shown to modify vertical PV distributions, where the diabatic heating due to condensation via cloud processes, as induced by strong ascent, gives rise to PV-production below and destruction above a center of diabatic heating (e.g., Wernli and Davies, 1997; Wernli, 1997; Madonna et al., 2014). The outflow of low-PV air in the upper-troposphere, as followed by this vertical PV modification, helps to create and maintain the upper-level block.

Table S5: Additional information for Ural blocking heated trajectories belonging to each sub-selection based on pressure criteria as given in the first column: considering only the maximum ascent within 48 h (ΔP_{48h}) or with an additional pre-criterion of considering only trajectories that at some point experience a pressure above 790 hPa. The percentages in the column "% of Heated" show the relative fraction of all original heated trajectories satisfying the criterion, comparable to the absolute number of trajectories given in the column next to the criterion. The relative percentages of trajectories satisfying the criterion within the main heating domain (A) or outside the domain (O) are also shown (sum over the last two rows equals 100 %).

Selection	**Amount of Heated traj.**	**% of Heated**	**A (%)**	**O (%)**
$\Delta P_{48h} \geq 0$ hPa	57323	100	68	32
$\Delta P_{48h} \geq 300$ hPa	38099	66	71	29
$\Delta P_{48h} \geq 400$ hPa	23623	41	76	24
$\Delta P_{48h} \geq 500$ hPa	11677	20	80	20
$\Delta P_{48h} \geq 600$ hPa	3197	6	86	14
$P \geq 790$ hPa & $\Delta P_{48h} \geq 0$ hPa	31275	55	73	27
$P \geq 790$ hPa & $\Delta P_{48h} \geq 300$ hPa	26965	47	74	26
$P \geq 790$ hPa & $\Delta P_{48h} \geq 400$ hPa	20747	36	77	23
$P \geq 790$ hPa & $\Delta P_{48h} \geq 500$ hPa	11489	20	80	20
$P \geq 790$ hPa & $\Delta P_{48h} \geq 600$ hPa	3197	6	86	14

Regarding the strong criterion of ascent within two days, we observe that the heated trajectories originating both from Ural and Scandinavian blocks (Fig. 8e, f, in red) experience a median ascent of 363 and 309 hPa, respectively, where only the 95$^{\text{th}}$ whisker extends until 600 hPa. This already suggests that the heated blocking trajectories in general experience weaker ascent, however still strong enough for PV modification and transport of low-PV air into the upper-level blocking regions, as explained above.

The selection criteria used in this section are listed in the first column in Table S5. The percentages given in the third column show the relative fractions of the originally defined heated Ural blocking trajectories that fulfill the selection criterion. The first row having an undefined magnitude of ascent results in selecting all 57323 heated trajectories defined for the Ural events (58 % of all Ural blocking trajectories), which is seen by a percentage of 100 % and the same relative fractions for the heating domains as discussed in Sect. 5.1.

Figure S1 shows the vertical distribution of pressure at 12-hourly steps for four days around the time of maximum heating (red box), shown for heated trajectories experiencing maximum heating within the main domain (A) or outside (O) and fulfilling the additional criteria. Starting with the simple criterion of restricting, for each 6-day heated trajectory, the ascent within 48-hours to exceed 0, 300, 400, 500 or 600 hPa, respectively, (Fig. S1 two first rows) we observe that the stronger the ascent criterion, the smaller the fraction of the heated trajectories will fulfill it, resulting in only 6 % for the strongest ascent criterion of 600 hPa (last column). Having in mind that these identified upper-level Ural blocks mainly reside north of the Urals in higher latitudes, where the tropopause is usually lower, WCBs outflows may be less frequent in high-latitude regions, and thus, less of the Ural blocking trajectories may fulfill the WCBs criterion. Additionally, by a stricter ascending criterion, more of the selected

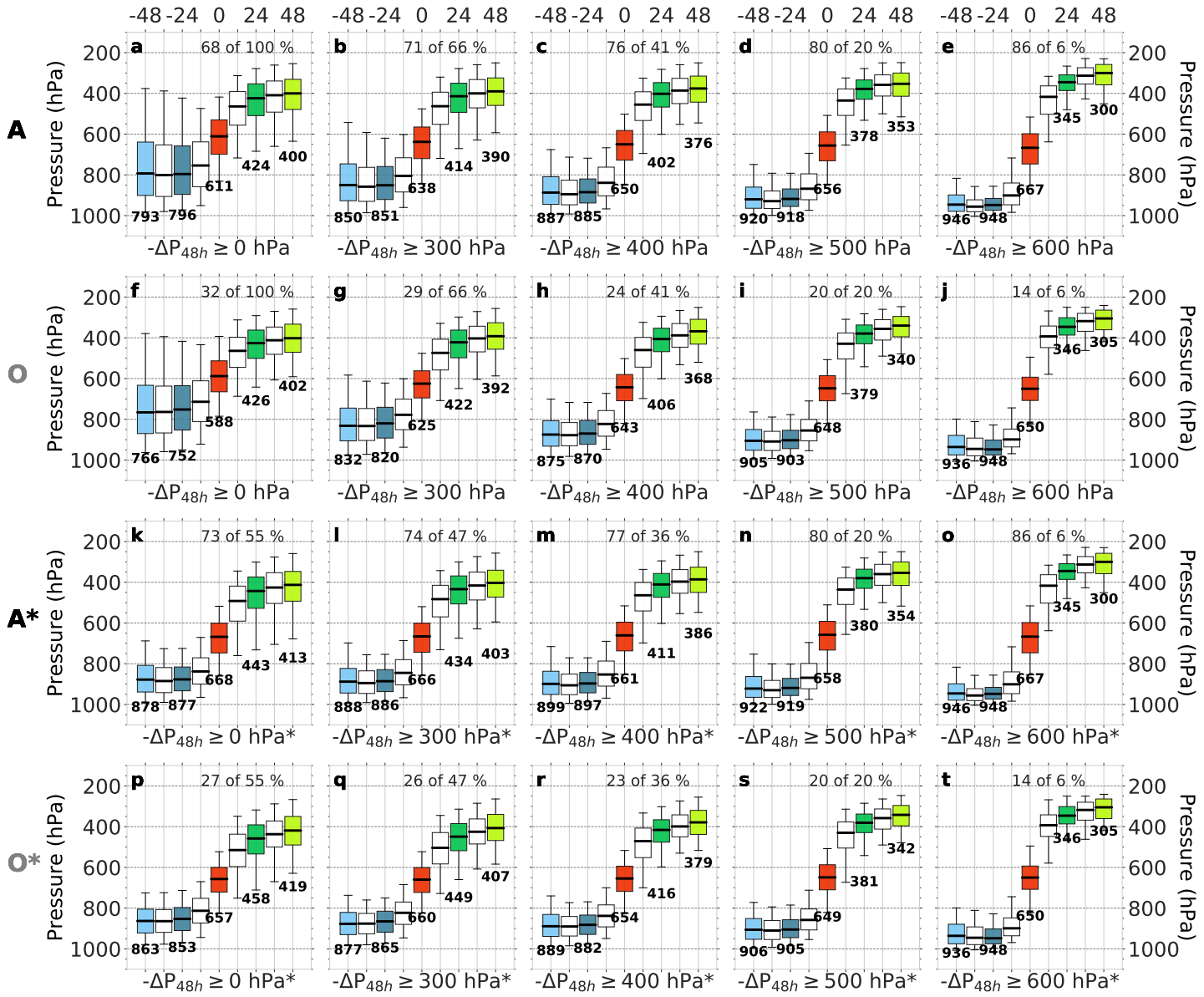

Figure S1: Evolution of pressure along trajectories at 12-hourly steps relative to the time of maximum heating within the heating domains: main domain A and A* (first and third row) and outside the region O and O* (second and last row), where the star denotes the additional pressure criterion of obtaining a pressure ≥ 790 hPa. The sub-selection of the heated trajectories is based on the additional ascent criterion of $\Delta P_{48h} \geq 0$ hPa (first column), 300 hPa (second column), 400 hPa (third column), 500 hPa (fourth column) and 600 hPa (last column), respectively. Median value per 24-hourly time slots are shown in text and as horizontal lines, boxes denote the interquartile range and whiskers show the 5^{th} – 95^{th} percentile range. The colors of the boxes are consistent with the colors used in Fig. 11. The relative percentage of all heated trajectories satisfying the criterion is given on the top of each panel, as also listed in Table S5.

trajectories experience maximum heating in the North Atlantic domain (A, first row), reaching up to a relative percentage of 86 % with the strongest criterion (Fig. S1e).

With a stronger ascent criterion, the absolute difference between the time of maximum heating (red) to each 12 h time steps back- and forwards becomes larger, as expected, the median pressure at maximum heating increases, the spread between the pressures at each time slot decreases and the the outflow in the upper troposphere reaches lower pressure levels. The behaviour between the first and second rows in Fig. S1 are rather similar with only slight discrepancies.

Similar changes regarding the relative fractions and vertical pressure evolution are found by stronger criterion

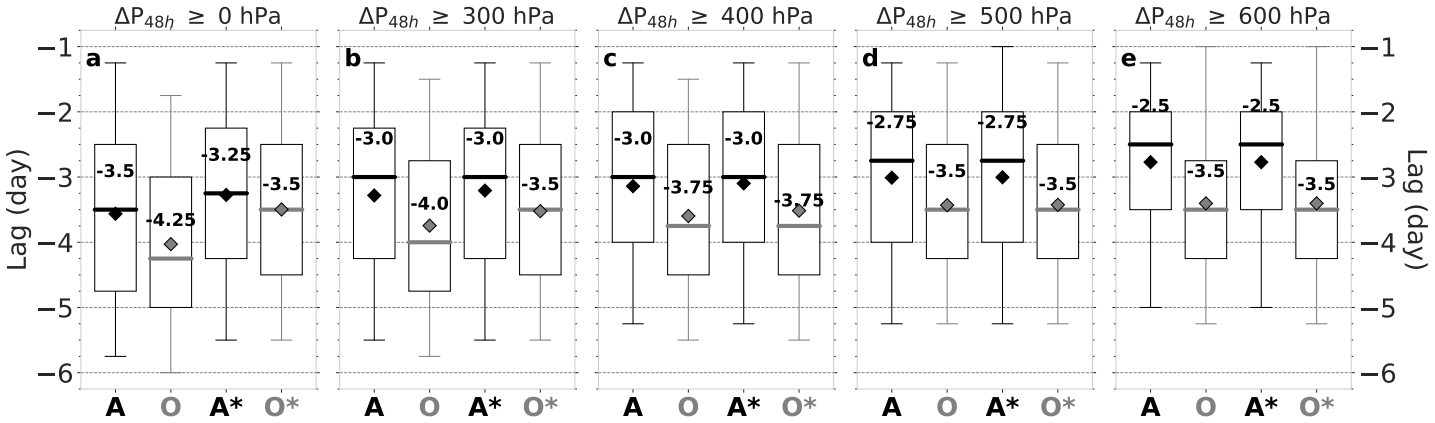

Figure S2: Statistical distributions of the time lags, relative to trajectory initialization, at maximum heating in the main North-Atlantic domain (A, black) or outside the region (O, gray), shown for heated Ural blocking trajectories satisfying an additional ascent criterion of -$\Delta P_{48h} \geq 0$ hPa (a), -$\Delta P_{48h} \geq 300$ hPa (b), -$\Delta P_{48h} \geq 400$ hPa (c), -$\Delta P_{48h} \geq 500$ hPa (d) and -$\Delta P_{48h} \geq 600$ hPa (e). The upper-star (*) for the third and fourth boxplots in each subplot denotes the selection of trajectories that satisfy an additional pre-criterion of at some time before the ascent residing at the surface ($P \geq 790$ hPa). Each box shows the interquartile range, the whiskers mark the 5^{th} - 95^{th} percentile range, the median lag is shown both in text and by the colored horizontal line and the diamond marks the mean. The relative percentages within each selection criterion are listed in Table S5.

when including trajectories originated below 790 hPa before applying the ascent criterion. The relative fractions for each of the criterion are listed in the second group of rows in Table S5. When including trajectories residing in the lowermost troposphere without any additional ascent criterion (Fig. S1k, p), only 55 % of all heated trajectories get selected. Already at this selection stage, relatively more of the trajectories get heated in the A domain (A* (compare Fig. S1k with Fig. S1a). Note that trajectories fulfilling the first criterion (Fig. S1e) equals the chosen trajectories satisfying the additional criterion (Fig. S1o), showing that trajectories experiencing strong ascent of more than 600 hPa within two days automatically at some point of their journey reside in the lowermost troposphere, i.e., fulfill the definition of WCBs.

Not only does the North Atlantic heating domain become more dominant, but also the lag of maximum heating by stronger ascent criterion gets shifted to later lags (closer to the block), being more pronounced for trajectories experiencing maximum heating in the main region. Figure S2 shows the statistical distributions of the temporal location of maximum heating in the main North-Atlantic region (A, black) or outside the region (O, gray), for both criteria used here. Figure S2a equals the distribution discussed in Sect. 5.1 for the first criterion (compare also with Fig. 12b). We observe a one day shift from a median lag of −3.5 day to −2.5 day by stronger ascent criterion for the A domain, whereas a shift to later lags by stronger criterion is also noticeable for trajectories experiencing maximum heating outside the main region. When applying the additional pressure criterion (*), a similar shift to later lags is visible, though rather unchanged for the O* regions.

Even though less trajectories are selected when adding selection criterion based on pressure changes or absolute value of pressure prior to ascent, the general pattern in the pressure evolution with respect to maximum heating remains the same for all selections. The only remarkable changes are the shift of maximum heating to later lags, relatively more trajectories experience heating in the main North Atlantic domain and the absolute pressure difference between the time of maximum heating and its near timesteps increases when applying additional, stronger ascent criterion.

References

Madonna, E., Wernli, H., Joos, H., and Martius, O. (2014). Warm conveyor belts in the ERA-Interim dataset (1979–2010). Part I: Climatology and potential vorticity evolution. *J. Climate*, 27(1):3–26.

Wernli, B. H. and Davies, H. C. (1997). A Lagrangian-based analysis of extratropical cyclones. I: The method and some applications. *Q. J. Roy. Meteor. Soc.*, 123(538):467–489.

Wernli, H. (1997). A Lagrangian-based analysis of extratropical cyclones. II: A detailed case-study. *Q. J. Roy. Meteor. Soc.*, 123(542):1677–1706.